








RESEARCH ARTICLE

Biphasic calcium phosphate with submicron surface topography in an *Ovine* model of instrumented posterolateral spinal fusion

Lukas A. van Dijk^{1,2}  | Rongquan Duan^{1,3}  | Xiaoman Luo¹ | Davide Barbieri¹ | Matthew Pelletier⁴  | Chris Christou⁴  | Antoine J. W. P. Rosenberg² | Huipin Yuan^{1,5}  | Florence Barrère-de Groot¹ | William R. Walsh⁴  | Joost D. de Bruijn^{1,6} 

¹Kuros Biosciences BV, Bilthoven, The Netherlands

²Department of Oral and Maxillofacial Surgery, University Medical Center Utrecht, Utrecht, The Netherlands

³Biomaterial Science and Technology, University of Twente, Enschede, The Netherlands

⁴Surgical and Orthopaedic Research Laboratories, Prince of Wales Clinical School, University of New South Wales, Sydney, New South Wales, Australia

⁵MERLN Institute for Technology-inspired Regenerative Medicine, Maastricht University, Maastricht, The Netherlands

⁶School of Materials Science and Engineering, Queen Mary University of London, London, UK

Correspondence

Joost D. de Bruijn, School of Materials Science and Engineering, Queen Mary University of London, UK.

Email: j.d.debruijn@qmul.ac.uk

Funding information

Horizon 2020, Grant/Award Number: 674282

As spinal fusions require large volumes of bone graft, different bone graft substitutes are being investigated as alternatives. A subclass of calcium phosphate materials with submicron surface topography has been shown to be a highly effective bone graft substitute. In this work, a commercially available biphasic calcium phosphate (BCP) with submicron surface topography (MagnetOs; Kuros Biosciences BV) was evaluated in an *Ovine* model of instrumented posterolateral fusion. The material was implanted stand-alone, either as granules (BCP_{granules}) or as granules embedded within a fast-resorbing polymeric carrier (BCP_{putty}) and compared to autograft bone (AG). Twenty-five adult, female Merino sheep underwent posterolateral fusion at L2-3 and L4-5 levels with instrumentation. After 6, 12, and 26 weeks, outcomes were evaluated by manual palpation, range of motion (ROM) testing, micro-computed tomography, histology and histomorphometry. Fusion assessment by manual palpation 12 weeks after implantation revealed 100% fusion rates in all treatment groups. The three treatment groups showed a significant decrease in lateral bending at the fusion levels at 12 weeks ($P < 0.05$) and 26 weeks ($P < 0.001$) compared to the 6 week time-point. Flexion-extension and axial rotation were also reduced over time, but statistical significance was only reached in flexion-extension for AG and BCP_{putty} between the 6 and 26 week time-points ($P < 0.05$). No significant differences in ROM were observed between the treatment groups at any of the time-points investigated. Histological assessment at 12 weeks showed fusion rates of 75%, 92%, and 83% for AG, BCP_{granules} and BCP_{putty}, respectively. The fusion rates were further increased 26 weeks postimplantation. Similar trends of bone growth were observed by histomorphometry. The fusion mass consisted of at least 55% bone for all treatment groups 26 weeks after implantation. These results suggest that this BCP with submicron surface topography, in granules or putty form, is a promising alternative to autograft for spinal fusion.

KEYWORDS

biphasic calcium phosphate, posterolateral spinal fusion, sheep, submicron, surface topography

1 | INTRODUCTION

The annual number of spinal fusion procedures in the US for the treatment of degenerative spine conditions has risen rapidly over the past two

decades to >770,000.¹ The most commonly used spinal fusion technique is posterolateral fusion (PLF), which is either performed as an individual procedure (19%) or in combination with interbody cage fusion (45%).² Because these procedures require large volumes of bone graft

(12-36 cc),³ bone graft substitutes are frequently employed to reduce or avoid morbidity related to the harvesting of autologous bone.⁴ Calcium phosphate-based bone grafts have been widely investigated because of their excellent biocompatibility, osteoconductivity and controllable resorption rate.⁵ A commonly addressed disadvantage compared to autologous bone is their lack of osteogenic and osteoinductive capacity. However, efforts to modify the physicochemical properties of calcium phosphates (ie, composition, porosity and, most recently, surface properties) have resulted in materials with bone-inducing properties. In particular, submicron surface topographies have been reported to enhance angiogenesis and bone healing properties following *in vivo* implantation.⁵⁻⁸

Surface properties of biomaterials have been shown to influence the phenotype of macrophages,⁹⁻¹¹ that are key modulators in the foreign body and wound healing responses.^{12,13} For promotion of bone repair, an increase in anti-inflammatory macrophages following an initial phase with pre-dominantly pro-inflammatory macrophages has been suggested to be important.^{14,15} Recently, calcium phosphates with submicron surface topography have been shown to promote the transition of macrophages to the pro-healing, anti-inflammatory M2 phenotype *in vitro*,⁸ which has been linked to enhanced angiogenesis and superior bone healing properties observed with these materials.^{6,7}

In the current study, a clinically relevant¹⁶⁻¹⁸ *Ovine* model of instrumented PLF was used to compare treatment outcomes of a biphasic calcium phosphate (BCP) with submicron surface topography to bone autograft as a stand-alone treatment. The bone graft was implanted as granules alone and as a putty, with granules embedded in a fast-resorbing polymeric binder designed to improve handling properties. Study endpoints included fusion rate by manual palpation, range of motion (ROM), histology and histomorphometrical analysis of bone in the fusion mass after 6, 12 and 26 weeks.

2 | METHODS

2.1 | Calcium phosphate

Commercially available BCP bone graft (MagnetOs; Kuros Biosciences BV, Bilthoven, Utrecht, the Netherlands) was provided as granules (BCP_{granules}) and putty (BCP_{putty}). Both formulations contain 1 to 2 mm granules of bioactive bone graft comprising 65% to 75% Tri-Calcium Phosphate (TCP—Ca₃(PO₄)₂) and 25% to 35% Hydroxyapatite (HA—Ca₁₀(PO₄)₆ (OH)₂). The carrier in the putty formulation is a tri-block copolymer synthesized from polyethylene glycol (PEG) and L-lactide monomer. The resulting polymer is water-soluble and dissolves at near body temperature, leading to rapid dispersion after implantation (<48 hours).¹⁹ Scanning electron microscopy (SEM; JSM 5600, JEOL) was used to characterize the submicron surface topography. Bioactivity of the BCP surface was evaluated *in vitro* using the validated assay described by Kokubo et al.²⁰ Briefly, the materials were submerged in simulated body fluid (SBF) for 2, 4, 7, and 10 days and subsequently analyzed for presence of an apatite-like-layer using SEM. The materials for the animal study were provided sterile having been sterilized by gamma irradiation (25 kGy).

2.2 | Animal study

The study design was based on a previously reported sheep model of PLF^{18,21,22} and was approved by the local Animal Care and Ethics Committee (ACEC). Surgery was performed on 25 adult, female Merino sheep (4-5 years, 80-90 Kg, at the University of New South Wales [UNSW], Australia). Animals were randomly distributed into three groups for the 6, 12, and 26-week time-points, with an *n* of 8, 9, and 8, respectively. Preoperative, animals were administered fentanyl (2 µg/kg/h, t.d.), buprenorphine (0.006 mg/kg, s.c.) and Carprofen (4 mL, s.c.) for pain relief and Zoletil (8-12 mg/kg, i.m.) for induction. Anesthesia was achieved and maintained by isoflurane (2%-4% in 100% O₂). Surgery consisted of multi-level instrumented spinal PLF procedure at levels L2-L3 and L4-L5. In short, facet joints and transverse processes (TPs) were exposed followed by destabilization of the motion segments and excision of the facet joints, spinous processes and ligaments. TPs were decorticated after which the operative levels were bilaterally instrumented with polyaxial pedicle screws (Ø 5.0 × 35 mm) and titanium rods (Ø 5.5 mm, Wiltrom Co., Ltd., Zhubei City, Hsinchu County, Taiwan). Subsequently, 20 cc of graft material was equally distributed to the bilateral arthrodesis sites in direct apposition with each of the TPs (10 cc per side). The three graft materials were iliac crest- and proximal tibia-derived (1:1) autologous bone graft (AG), BCP_{granules}, and BCP_{putty}, randomly allocated to the fusion levels (*n* = 5 for 6 and 26 weeks, *n* = 6 for 12 weeks). Postsurgery, the animals were housed at the laboratory animal facility where they were monitored and received proper postoperative care. After 6, 12, and 26 weeks, animals were euthanized by IV injection of Lethotarb (1 mL/2 kg i.v., 325 mg/mL) for analyses of endpoints.

2.3 | Manual palpation

After euthanasia, harvesting of the spines and removal of pedicle rods, the L2-L3 and L4-L5 segments were manually subjected to flexion-extension (FE) and lateral bending (LB) to assess spine mobility. All levels were graded as either fused (low mobility), partially fused (one-sided mobility) and not fused (high mobility) under FE and LB. The fisher-Freeman-Halton Exact Test was performed for statistical analysis (*P* < 0.05).

2.4 | Micro-computed tomography

Micro-computed tomography (micro-CT) was performed using an Inveon Scanner (Siemens Medical Solutions USA, Inc., Knoxville, TN, USA) at a slice thickness of 50 µm.

2.5 | Biomechanical analysis

The treated levels were separately mounted on a robotic six degree of Simulation Solutions Ltd., Stockport, UK freedom musculoskeletal simulator, simVITRO (Simulation Solutions Ltd., Stockport, UK and Cleveland Clinic Biorobotics Lab, Cleveland, OH, USA). A 7.5 Nm pure moment was applied to the segments in FE, LB and axial rotation (AR). Each loading profile was repeated three times for every specimen and the mean angular deformation was recorded. Data were analyzed with a two-factor ANOVA with a significance level of *P* < 0.05 using dedicated software (Graphpad version 5). Normal distribution of data was confirmed by Kolmogorov-Smirnov normality test.

2.6 | Histology and Histomorphometry

The treated spine levels were fixed in 4% phosphate-buffered formalin for 1 week at 4° Celsius. After fixation, samples were dehydrated through a series of increasing ethanol concentrations and were subsequently embedded in methacrylate. A Leica SP1600 saw-microtome was used to cut sagittal cross-sections (10-20 μm) from the region between TPs of each contralateral fusion mass. From each sample, three sections were obtained across the fusion mass for evaluation. Sections were stained with 1% methylene blue and 0.3% basic fuchsin to visualize bone tissue (bone matrix: pink, fibrous tissues: blue). Sections were visualized under a Leica microscope (Eclipse 50i, Nikon) for histological observation and were imaged using a slide scanner (DiMage scan 5400 Elite II, Konica Minolta, Tokyo, Japan) to obtain overviews for fusion assessment followed by histomorphometrical analysis. Each section was evaluated for histological fusion. Histological fusion was scored when a continuous presence of bone was observed between the TPs, connecting the adjacent spine segments.

From each fusion mass, the most representative section was used for histomorphometry. Histomorphometry of the fusion mass was performed by pseudo-coloring pixels representing bone and remaining implant material in a region of interest (Adobe Photoshop Elements 2.0). Values were expressed in mean and SD. For statistical evaluation, a two-factor ANOVA was performed ($P < 0.05$). Normal distribution of data was confirmed by D'Agostina-Pearson normality test.

3 | RESULTS

3.1 | Material characterization

Surface structure analysis of the porous BCP granules (Figure 1A) by SEM demonstrated a surface topography of submicron-scale polygon crystals (Figure 1B). Average surface crystal diameter was determined to be $0.58 \pm 0.21 \mu\text{m}$. Surface mineralization, evident from the development of an apatite-like-layer of globules, was

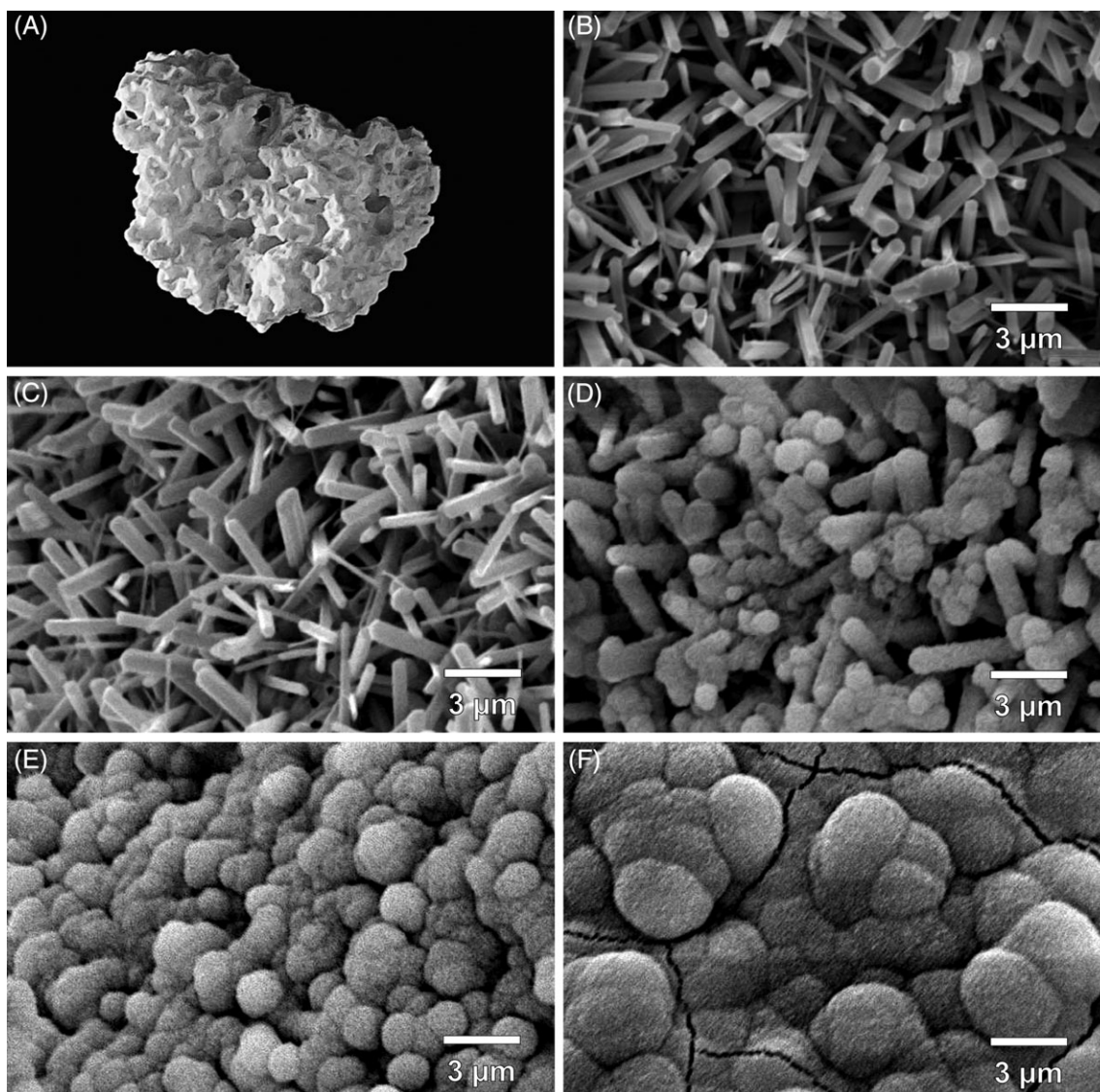


FIGURE 1 (A) Porous BCP granule of 1-2 mm in size with (B) submicron surface topography of epitaxial polygon crystals. Submersion in SBF resulted in the progressive formation of an apatite-like mineral layer on the material surface as shown by SEM after (C) 2 days, (D) 4 days, (E) 7 days, and (F) 10 days

observed in an increasing manner with time following submersion in SBF (Figure 1B-F). These results confirm the bioactivity of the BCP surface.

3.2 | Micro-computed tomography

Surgery and recovery proceeded without adverse events or adverse reactions to the implant materials. After 6, 12, and 26 weeks, animals were euthanized and the spine and surrounding tissues were harvested. Imaging by micro-CT showed that all graft materials were well-contained at the implantation sites and there was progression to a solid fusion mass between the spine segments over time (Figure 2). At 26 weeks, mature fusion masses were evident and were indicated by incorporation of the graft materials with host bone, and the inability to discriminate individual BCP particles. Evaluation of fusion masses suggested higher fusion mass volumes in the BCP groups at 12 and 26 weeks than with AG, indicating higher graft volume stability with the BCP treatments.

3.3 | Manual palpation

Results of fusion assessment by palpation in a blinded manner are presented in Table 1. The data indicate a 100% fusion rate in each group

TABLE 1 Fusion rate by manual palpation

Time-point	AG	BCP _{granules}	BCP _{putty}	P value ^a
6 weeks	3/5	1/5	1/5	0.50
12 weeks	6/6	6/6	6/6	0.99
26 weeks	5/5	5/5	5/5	0.99

^a Fisher-Freeman-Halton exact test.

from 12 weeks onwards. No partially fused spines were found by manual palpation. No statistically significant differences in fusion between treatments at each time-point were determined (Fisher-Freeman-Halton exact test, $P \geq 0.5$).

3.4 | Biomechanical evaluations

ROM testing was performed to determine whether treatment resulted in a reduction in mobility between the segments and thus a higher stability, which is the primary goal of spinal fusion. Results of ROM tests are presented in Figure 3. These results show decreasing trends in ROM in LB, FE, and AR with no differences between treatment groups. The decrease was strongest in LB for all materials, with an average decrease of $5.50^\circ \pm 1.59$ between 6 and

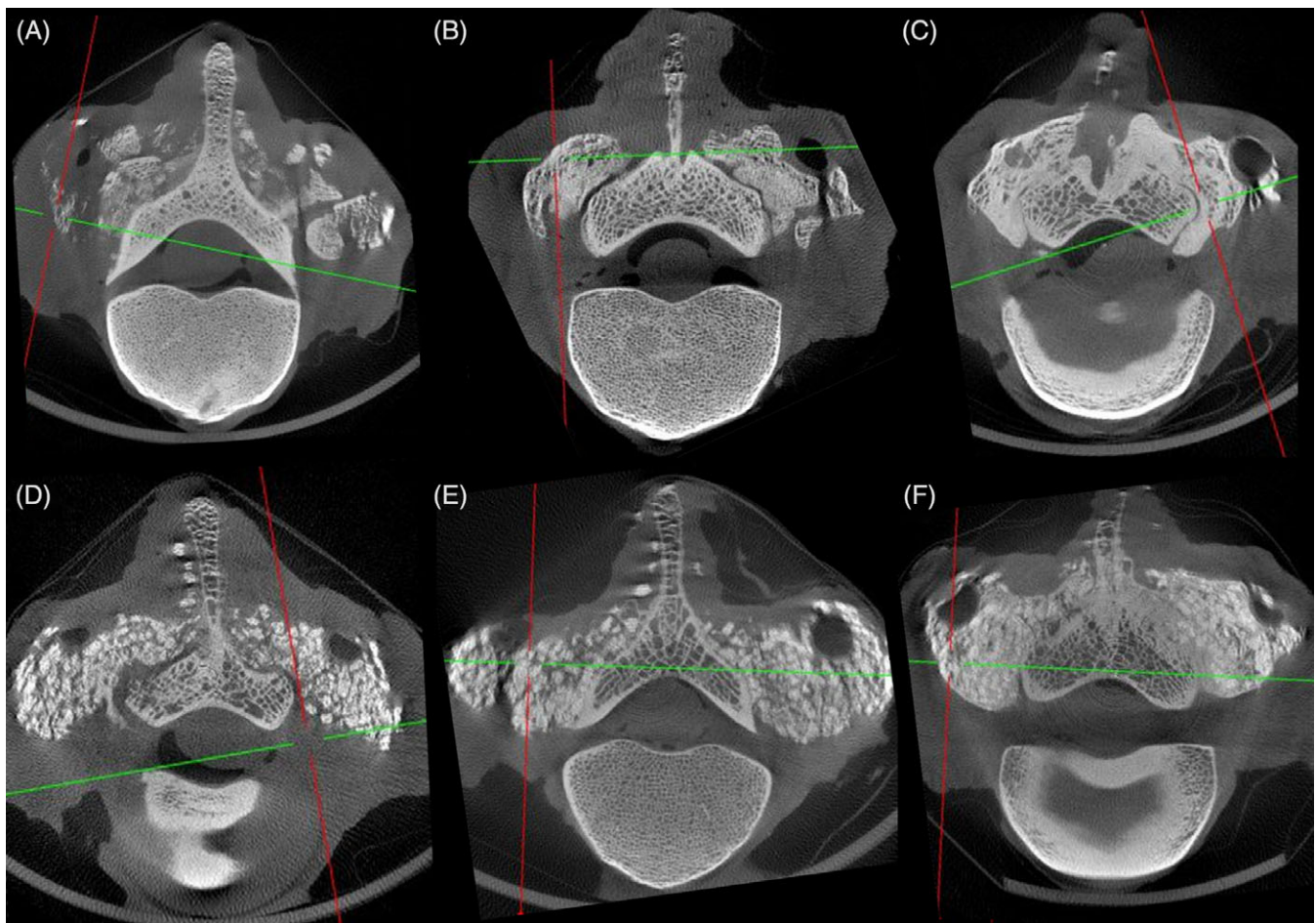


FIGURE 2 Examples of transversal micro-CT slices of the treated spine levels for AG (A-C) and BCP (D-F) at 6 (A, D), 12 (B, E) and 26 (C, F) weeks. During time, consolidation of the fusion mass was evident for all treatments and gradual integration of graft materials with the underlying host bone was observed. Graft volume at 12 and 26 weeks appear higher for BCP treatments than for AG, suggesting a higher graft volume stability for BCP

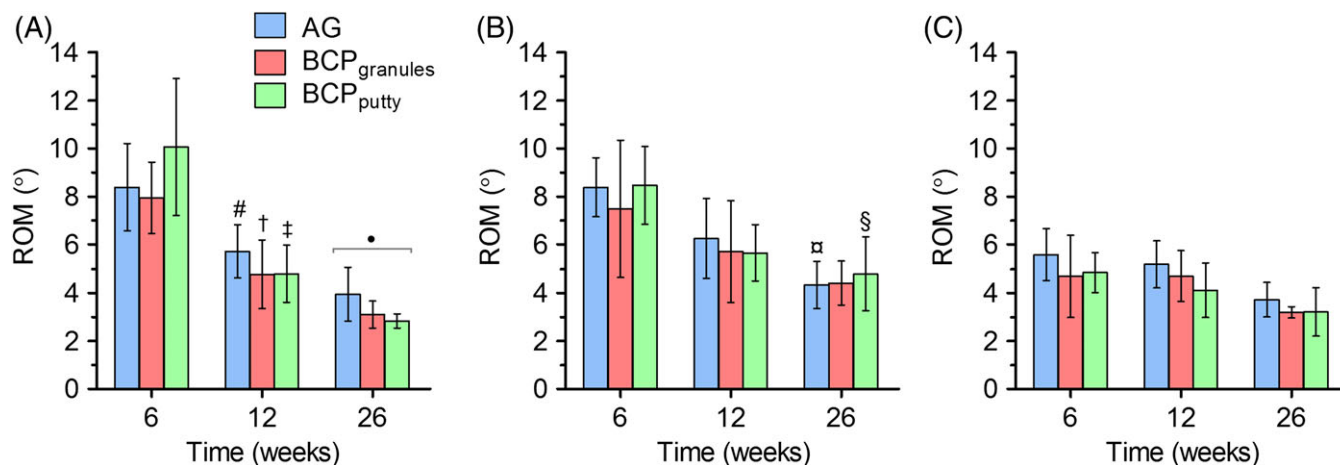


FIGURE 3 Diagrams presenting ROM data of treated segments in LB (A), FE (B) and AR (C). Decrease in ROM over time was evident for each loading direction, with no significant differences between groups. Symbols: # significantly different from AG, 6 weeks ($P < 0.05$); † significantly different from BCP_{granules}, 6 weeks ($P < 0.01$); ‡ significantly different from BCP_{putty}, 6 weeks ($P < 0.05$); • all significantly different from 6 weeks ($P < 0.001$); ¶ significantly different from AG, 6 weeks ($P < 0.01$); § significantly different from BCP_{putty}, 6 weeks ($P < 0.05$)

26 weeks and statistical significance between 6 weeks and the later time-points (two-factor ANOVA, $P < 0.05$). In FE, the average decrease was $3.60^{\circ} \pm 1.65$ between 6 and 26 weeks, with significance for AG and BCP_{putty}, but not for BCP_{granules}. Although the data for AR show a slight decrease in ROM of an average $1.67^{\circ} \pm 1.03$ between 6 and 26 weeks, statistical significance was not reached. No statistical differences between graft materials were seen in any loading direction at any time-point, indicating equivalent spinal stability between the positive control, autograft, and the treatment groups, BCP_{putty} and BCP_{granules}.

3.5 | Histology and histomorphometry

All further evaluations were performed by histology. Presence of a bony fusion between the segments was assessed on sagittal cross-sections of the fusion mass, as presented in Figure 4. The fusion scores are given in Table 2. As the data show, fusion was rarely observed at 6 weeks. However, a steep increase was observed for all treatments at 12 weeks, with fusion rates of 75%, 92%, and 83% for

AG, BCP_{granules} and BCP_{putty}, respectively. Specimens of the 26-week endpoint showed a further increase in percentage of segments fused with 90%, 100% and 90% for AG, BCP_{granules} and BCP_{putty}, respectively. Differences in fusion rate between treatments were not of statistical significance, indicating equivalent performance between the three graft materials (Fisher-Freeman-Halton exact test, $P \geq 0.05$).

High and low magnification histological sections were examined to evaluate tissues within the fusion mass (Figures 4 and 5). Fibrous tissue and blood vessel infiltration was complete in the central region of the fusion at week 6 in all implants. In addition, bone formation was observed near the host bone bed after 6 weeks in all groups. During the healing period, progression of bone tissue throughout the fusion mass was observed, with an increased proportion of bone at 12 weeks and bone tissue occupying the full range of the fusion mass after 26 weeks. Bone tissue was observed growing directly on BCP material surface, with cuboidal osteoblasts colonizing the material surface and secreting osteoid. Maturation of bone tissue in the fusion mass was indicated by the transition from an early bone phenotype

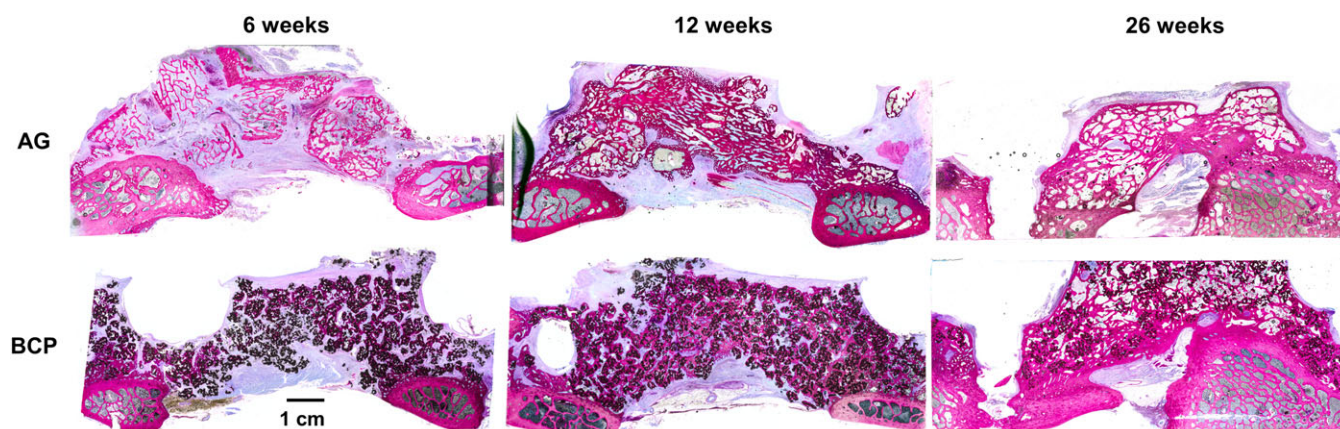


FIGURE 4 Sagittal histological sections (basic fuchsin-methylene blue) of spine levels grafted with AG or BCP, taken from the region between the TP's. These sections were used to score spinal fusion, that is, the presence of a continuous bone bridge between the adjacent transverse processes. The 6 weeks sections shown on the left were scored as "not fused" whereas 12 and 26 weeks shown in the center and right side were scored as "fused". Fusion by histology was frequently observed from 12 weeks onwards

TABLE 2 Fusion rate by histology

Time-point	AG			BCP _{granules}			BCP _{putty}			P value ^a
	U	B	FR (%)	U	B	FR (%)	U	B	FR (%)	
6 weeks	1/5	0/5	10	0/5	0/5	0	0/5	0/5	0	0.99
12 weeks	1/6	4/6	75	1/6	5/6	92	2/6	4/6	83	0.85
26 weeks	1/5	4/5	90	0/5	5/5	100	1/5	4/5	90	0.99

Abbreviations: B, bilateral fusion; FR, fusion rate; U, unilateral fusion.

^a Fisher-Freeman-Halton exact test.

with abundant osteoid, woven bone and fibrous tissue towards a mature bone phenotype at 26 weeks, characterized by a large proportion of lamellar bone and bone marrow. Osteoclast-like multinucleated phagocytes were observed phagocytosing the BCP material indicating the cell-mediated resorption of the implanted material. Gradual degradation of BCP granules was evident by the presence of small particles of BCP separated from larger granules up to the 26-week time-point.

Histomorphometry data, represented in Figure 6, are consistent with the general histological observation of the fusion mass. In all groups, the proportion of bone in the fusion mass steadily increased over time in a significant trend ($P < 0.001$), leading up to over 55% of bone after 26 weeks. Between groups, at the 6-week time-point, a higher proportion of bone was determined in the AG group ($25.2\% \pm 5.0$) compared to BCP_{granules} ($14.8\% \pm 7.1$, $P < 0.01$) and BCP_{putty} ($10.8\% \pm 5.9$, $P < 0.001$), which can be explained by the presence of autologous bone chips that were implanted at the fusion site. After healing periods of 12 and 26 weeks, no differences in bone volume were observed between all treatments ($P > 0.05$).

The proportion of BCP graft in the fusion mass was determined for BCP_{granules} and BCP_{putty} (Figure 6). As is evident from the graph, a decrease in material volume was determined over time. In both BCP groups, the amount of material in the fusion mass decreased by $\pm 25\%$ in the healing period from 6 weeks to 26 weeks, which was confirmed by statistical analysis ($P < 0.001$). No significant difference in material decrease between 6 and 12 weeks was determined for BCP_{granules} and BCP_{putty}. A slightly higher proportion of BCP graft in the fusion mass was seen for BCP_{putty} compared to BCP_{granules} at 6 weeks ($39.7 \pm 4.1\%$ vs $33.2 \pm 5.7\%$, $P < 0.01$) and 26 weeks ($29.9\% \pm 3.2$ vs $24.9 \pm 5.0\%$, $P < 0.05$).

4 | DISCUSSION

The posterolateral spine environment is known to be challenging for bone graft substitute materials because it provides very limited contact with host bone from which bone growth can progress. In fact, a successful lumbar arthrodesis is achieved by controlled bone

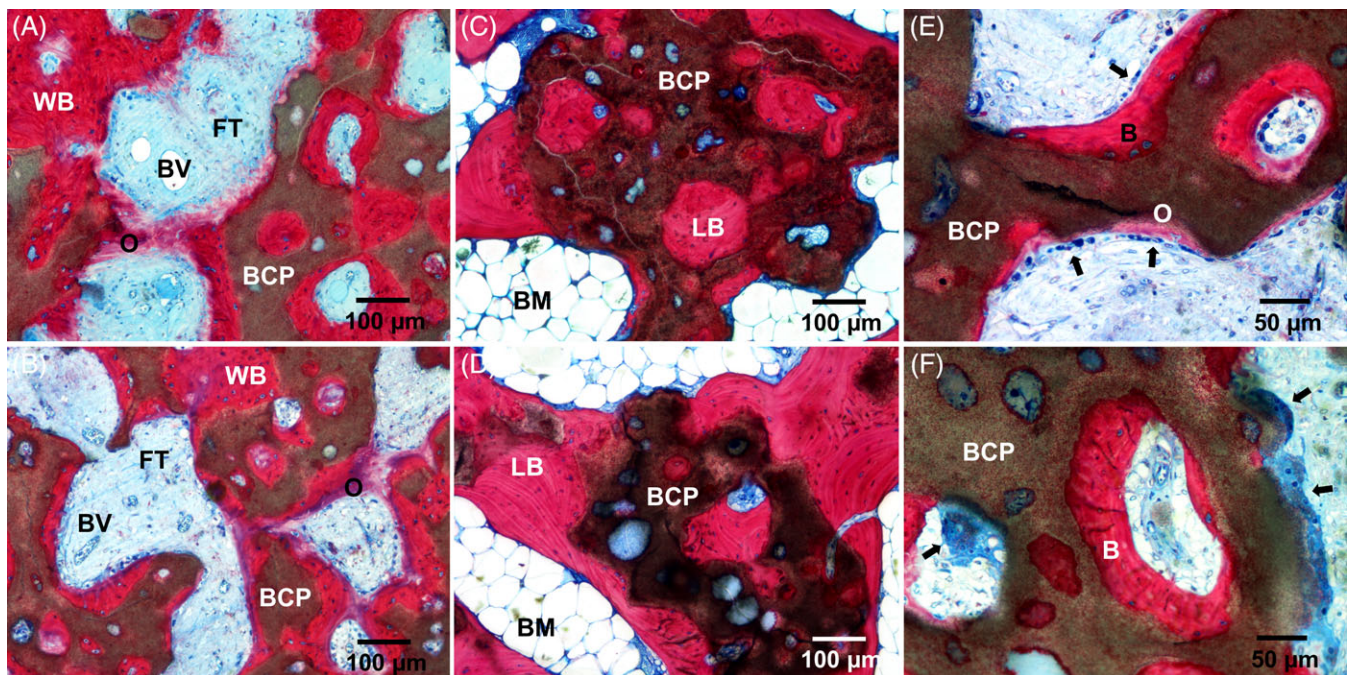


FIGURE 5 High magnification histology (basic fuchsin-methylene blue) of the grafts of levels treated with BCP_{granules} (A, C, E) and BCP_{putty} (B, D, F). Images show the progression and maturation of bone tissue from 6 weeks (A, B) to 26 weeks (C, D). Less mature bone tissue at 6 weeks is recognized by the presence of abundant fibrous tissue (FT), osteoid (O) and woven bone (WB). New bone tissue was observed forming around the BCP particles (BCP). At 26 weeks, more mature bone was recognized by the presence of lamellar bone (LB) and bone marrow (BM). Cuboidal osteoblasts were observed depositing osteoid directly on the BCP granule surface (E, arrows, 6 weeks). In addition, large multinucleated cells were observed resorbing the BCP material, with internalized fragments of material being apparent (F, arrows, 6 weeks)

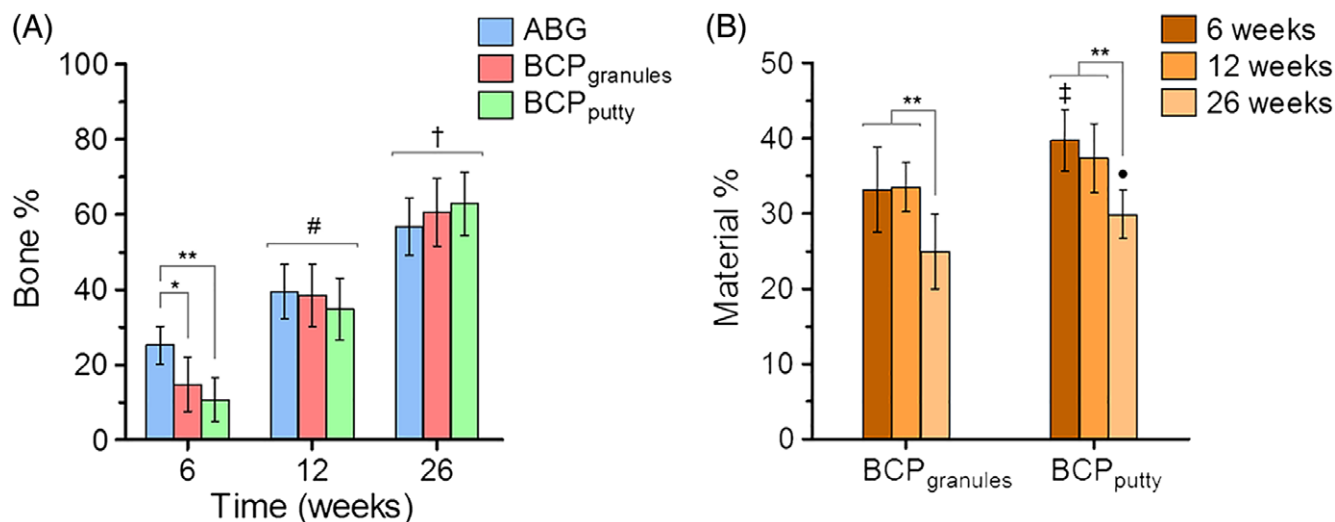


FIGURE 6 Diagrams presenting histomorphometry results of bone tissue (A) and BCP material (B) in the FM of the treated spine segments. Data are presented as percentage of the available space in a region of interest. A linear increase of bone tissue in the fusion mass during time is evident for all treatments (A). At 6 weeks, a slightly higher percentage of bone is shown for AG, but no differences were observed at later time-points. A decrease in material percentage during time was observed for both BCP treatments (B). A slight difference between BCP_{granules} and BCP_{putty} is apparent at 6 weeks and 26 weeks. Symbols: * $P < 0.01$; ** $P < 0.001$; # all significantly different from 6 weeks, $P < 0.001$; † all significantly different from 12 weeks and 6 weeks, $P < 0.001$; ‡ significantly different from BCP_{granules}, 6 weeks, $P < 0.01$; • significantly different from BCP_{granules}, 26 weeks, $P < 0.05$

formation through the paraspinous soft tissues in between adjacent TPs.²³ Because of this, materials with physicochemical properties designed to beneficially control the foreign body and wound healing responses may be more effective bone graft substitutes for PLF, as these can promote bone formation in sites distant from native bone through mechanisms other than osteoconduction alone.

Although most commercially available bone grafts have undergone testing in lapine posterolateral fusion studies, only a handful have been tested in higher-order animals such as sheep using posterior pedicle screws and rods. Wheeler et al.²⁴ compared BCP (Mastergraft; 15% HA/85% β -TCP) and autograft, and reported 57.1% and 100% fusion respectively at 16 weeks. Bone proportion in the fusion mass at 16 weeks was significantly lower for the BCP ($36.2\% \pm 3.95$) than for autograft ($55.1\% \pm 7.59$). In another work, that studied macroporous BCP (MBCP; 65% HA/35% TCP), Guigui et al.²⁵ reported that this material achieved fusion after 12 months while fusion by autograft was already observed after 6 months, as was confirmed by biomechanical testing. A third study by Baramki et al.²⁶ reported high fusion rates for autograft and interconnected porous HA after 20 weeks, but mechanical tests revealed poorer outcomes for the HA group. In the absence of posterior fixation, β -TCP alone has also shown inferior performance to autograft.²⁷ Other studies have reported more favorable outcomes for ceramics compared to autograft in this model,^{28–30} although certain limitations to those studies are evident when compared to the current work. First of all, fusion assessment by radiography (ie, X-ray and micro-CT) for evaluation of calcium phosphate grafts is inconclusive and may lead to overestimations, because the high radiopacity of calcium phosphate limits the ability to distinguish bone from material.^{31–33} Since the formation of bone tissue is crucial for a successful spinal fusion, fusion assessment by histology is a more accurate and reliable indicator than radiographic assessment. Moreover, studies described in the prior art

lacked internal references for mechanical testing (eg, multiple time-points) and reported equivalent spinal fusion with autograft or ceramics at 16 weeks or later. Lastly, the age of the animal is often reported as “skeletally mature” rather than the specific age or age range. This is important, as fusion rates drop considerably for 5-year-old ewes³⁴ as compared to 2-3-year-old ewes,³⁵ both of which are skeletally mature. The 4 to 5-year-old sheep used in the present study present an additional relevant challenge for the graft to overcome.

In the current work, by a combination of histological fusion data and mechanical data (ie, manual palpation and ROM testing) at multiple time-points, we demonstrated high spinal fusion success and equivalence to autograft as early as 12 weeks post-surgery by this BCP with submicron surface topography in both granule and putty form. Both BCP formulations showed equivalent and sustained efficacy for each endpoint, which indicates that the polymeric binder did not inhibit bone-healing performance of the granules. This is in line with expectations, since the binder was designed to rapidly dissolve after implantation and consists of a biologically inert composition. By histomorphometry at 6 weeks, levels treated with autograft showed a slightly but significantly larger proportion of bone tissue in the fusion mass, which may be explained by grafted autologous bone chips being included in the measurement of newly formed bone. Although manual palpation results suggest a higher fusion rate with autograft at 6 weeks (nonsignificant), the ROM and histological fusion data indicate similar healing progress between BCP treatments and autograft at the earliest time-point.

In comparison to previous studies, which show either an inferiority of calcium phosphates compared to autograft or equivalence evidenced through weaker endpoints, we demonstrate equivalent performance of AG, BCP_{granules} and BCP_{putty} by an array of strong assessment methods. In clinical literature, we can find conflicting

evidence about the efficacy of calcium phosphate materials as bone graft materials for spine fusion.^{36,37} Physicochemical properties of biomaterials are rarely discussed in clinical literature and it is often overlooked that these properties strongly influence the performance of calcium phosphate bone graft materials. Indeed, during preclinical *in vivo* studies, grafts with optimized physicochemical properties have presented better outcomes than those with suboptimal properties. For instance, calcium phosphate phase composition,^{38–43} macroporosity^{44–50} (ie, macro-pore size and interconnectivity) and bioactivity⁵¹ have been directly related to the *in vivo* tissue response, neovascularization and bone-forming potential in ectopic and orthotopic sites.^{40–43} Moreover, presence of a submicron surface topography and micro-porosity has been linked to substantially enhanced bone-inducing properties of calcium phosphates.^{6,7}

One of the current hypotheses on the effectiveness of calcium phosphates with submicron topography involves the polarization of macrophages. Macrophages play a key role in the foreign body response and their reaction to medical implants is pivotal for the success or failure of an implant after implantation.⁵² Being of a plastic nature, uncommitted macrophages can polarize towards a pro-inflammatory phenotype (M1) or anti-inflammatory phenotype (M2) in response to external triggers, including tissue damage or the implantation of a biomaterial.^{13,53} Studies have suggested that an increase in anti-inflammatory M2 macrophages following an initial phase of M1-dominated inflammation results in enhanced vascularization and osteogenesis.^{14,15} Moreover, surface properties of biomaterials have been demonstrated to influence macrophage phenotype after implantation^{9–11} and recently, calcium phosphates with a submicron surface topography were shown to promote the transition of macrophages to the M2 phenotype *in vitro*.⁸ The upregulation of M2 macrophages by submicron structured calcium phosphates may explain the enhanced angiogenesis and superior bone healing properties observed with these materials *in vivo*,^{6–8} as well as the results obtained in the current work. However, the techniques used in the current study to assess bone formation and spinal fusion were not designed for macrophage characterization. The proposed mechanism remains to be further experimentally verified in future studies.

A limitation of the current study is that no materials with different surface topographies were compared. Therefore, a recommendation for future studies in this model is to include materials with no surface topography or with surface topographies of different geometries and dimensions (ie, supermicron scale), in order to isolate the effect of material surface topography on graft efficacy. In addition, with regard to mechanical testing, inclusion of a sham or “empty” control (ie, no graft material) and baseline measurements immediately after surgery would provide more insight on the effect of spinal fusion by these graft materials on spine ROM.

We may conclude that this study provides solid evidence of the adequate performance of a BCP with tailored physicochemistry as stand-alone alternative to autograft in a clinically relevant *Ovine* model of PLF. By application of reliable fusion assessment by histology and supporting analyses at relevant time-points, we demonstrated a high fusion rate after 12 weeks for this material, with overall equivalence to autograft in fusion rate, mechanical integrity and bone formation over the entire healing period of 26 weeks. These findings support

the premise that calcium phosphates with a submicron surface topography are highly effective bone graft substitutes for PLF and this justifies further clinical investigation of these materials.

ACKNOWLEDGEMENTS

This study was supported by the European Union's Horizon 2020 Research and Innovation program (grant agreement no. 674282) and Kuros Biosciences BV.

Author contribution

H.Y., F.B. de G., W.W., J.D. de B.: Research Design. L. van D., R.D., X.L., D.B., M.P., C.C., H.Y., W.W.: Data acquisition and analysis. L. van D., H.Y., F.B. de G., W.W., J.D. de B.: Data interpretation. L. van D., H.Y., F.B. de G., J.D. de B., A.R.: Drafting paper or revising it critically. All authors have read and approved the final submitted manuscript.

CONFLICTS OF INTEREST

This study was supported by Kuros Biosciences BV. L. van D., R.D., X.L., D.B., F.B. de G., H.Y., and J.D. de B. are employees, or former employees, of Kuros Biosciences BV. H.Y. and J.D. de B. are stockholders of Kuros Biosciences BV. C.C., M.P., A.R., and W.W. have nothing to disclose.

ORCID

Lukas A. van Dijk  <https://orcid.org/0000-0002-2018-4041>

Rongquan Duan  <https://orcid.org/0000-0003-0728-8337>

Matthew Pelletier  <https://orcid.org/0000-0003-1643-6696>

Chris Christou  <https://orcid.org/0000-0003-3231-0356>

Huipin Yuan  <https://orcid.org/0000-0003-3353-7122>

William R. Walsh  <https://orcid.org/0000-0002-5023-6148>

Joost D. de Bruijn  <https://orcid.org/0000-0003-0367-3633>

REFERENCES

1. Millennium Research Group. *Orthopedic Biomaterials | Medtech 360 | Market Analysis | US | 2017*. Toronto: Millennium Research Group; 2016.
2. Pannell WC, Savin DD, Scott TP, Wang JC, Daubs MD. Trends in the surgical treatment of lumbar spine disease in the United States. *Spine J*. 2015;15(8):1719-1727.
3. Carragee EJ, Comer GC, Smith MW. Local bone graft harvesting and volumes in posterolateral lumbar fusion: a technical report. *Spine J*. 2011;11(6):540-544.
4. Scheufler K-M, Diesing D. Use of bone graft replacement in spinal fusions. *Orthopade*. 2015;44(2):146-153.
5. Dorozhkin S. Calcium orthophosphate-based bioceramics. *Materials (Basel)*. 2013;6(9):3840-3942.
6. Habibovic P, Yuan H, van den Doel M, Sees TM, van Blitterswijk CA, de Groot K. Relevance of osteoinductive biomaterials in critical-sized orthotopic defect. *J Orthop Res*. 2006;24(5):867-876.
7. Yuan H, Fernandes H, Habibovic P, et al. Osteoinductive ceramics as a synthetic alternative to autologous bone grafting. *Proc Natl Acad Sci USA*. 2010;107(31):13614-13619.
8. Duan R, Zhang Y, van Dijk LA, et al. 2018. Relation between macrophage differentiation, angiogenesis and topology-directed Osteoinduction of calcium phosphate ceramics. Paper presented at: 64th

- Annual Meeting of the Orthopaedic Research Society, March 10–13, 2018; New Orleans, LA.
9. Hotchkiss KM, Reddy GB, Hyzy SL, Schwartz Z, Boyan BD, Olivares-Navarrete R. Titanium surface characteristics, including topography and wettability, alter macrophage activation. *Acta Biomater.* 2016;31:425-434.
 10. Luu TU, Gott SC, Woo BWK, Rao MP, Liu WF. Micro- and Nanopatterned topographical cues for regulating macrophage cell shape and phenotype. *ACS Appl Mater Interfaces.* 2015;7(51):28665-28672.
 11. Bota PCS, Collie AMB, Puolakkainen P, et al. Biomaterial topography alters healing in vivo and monocyte/macrophage activation in vitro. *J Biomed Mater Res Part A.* 2010;95A(2):649-657.
 12. Italiani P, Boraschi D. From monocytes to M1/M2 macrophages: phenotypical vs functional differentiation. *Front Immunol.* 2014;5:514.
 13. Klopfeisch R. Macrophage reaction against biomaterials in the mouse model—phenotypes, functions and markers. *Acta Biomater.* 2016;43:3-13.
 14. Loi F, Córdova LA, Zhang R, et al. The effects of immunomodulation by macrophage subsets on osteogenesis in vitro. *Stem Cell Res Ther.* 2016;7(1):15.
 15. Spiller KL, Nassiri S, Witherell CE, et al. Sequential delivery of immunomodulatory cytokines to facilitate the M1-to-M2 transition of macrophages and enhance vascularization of bone scaffolds. *Biomaterials.* 2015;37:194-207.
 16. Pearce AI, Richards RG, Milz S, et al. Animal models for implant biomaterial research in bone: a review. *Eur Cells Mater.* 2007;13:1-10.
 17. Mageed M, Berner D, Jülke H, Hohaus C, Brehm W, Gerlach K. Is sheep lumbar spine a suitable alternative model for human spinal researches? Morphometrical comparison study. *Lab Anim Res.* 2013;29(4):183-189.
 18. Kanayama M, Cunningham BW, Setter TJC, et al. Does spinal instrumentation influence the healing process of posterolateral spinal fusion? An in vivo animal model. *Spine (Phila. Pa. 1976).* 1999;24(11):1058-1065.
 19. Barrère-de Groot F, Barbieri D, Grijpma DW, de Bruijn JD. 2018. United States Patent No. US2018/0028720A1. Anhydrous Biocompatible Composite Materials.
 20. Kokubo T, Ito S, Huang ZT, et al. Ca, P-rich layer formed on high-strength bioactive glass-ceramic A-W. *J Biomed Mater Res.* 1990;24:331-343.
 21. Kanayama M, Cunningham BW, Weis JC, Parker LM, Kaneda K, McAfee PC. Maturation of the posterolateral spinal fusion and its effect on load-sharing of spinal instrumentation. An in vivo sheep model. *J Bone Joint Surg Am.* 1997;79(11):1710-1720.
 22. Walsh WR, Harrison J, Loeffler A, et al. Mechanical and histologic evaluation of Collagraft in an ovine lumbar fusion model. *Clin Orthop Relat Res.* 2000;375:258-266.
 23. Foster MR, Allen MJ, Schoonmaker JE, et al. Characterization of a developing lumbar arthrodesis in a sheep model with quantitative instability. *Spine J.* 2002;2(4):244-250.
 24. Wheeler DL, Lane JM, Seim HB, et al. Allogeneic mesenchymal progenitor cells for posterolateral lumbar spine fusion in sheep. *Spine J.* 2014;14(3):435-444.
 25. Guigui P, Hardouin P. Histologic and biomechanic evaluation of posterolateral arthrodesis using a biphasic ceramic of calcium phosphate as bone substitute. Experimental study with sheep. *Bull Acad Natl Med.* 2000;184(2):403-414.
 26. Baramki HG, Steffen T, Lander P, et al. The efficacy of interconnected porous hydroxyapatite in achieving posterolateral lumbar fusion in sheep. *Spine (Phila. Pa. 1976).* 2000;25(9):1053-1060.
 27. Pelletier MH, Oliver RA, Christou C, et al. Lumbar spinal fusion with β -TCP granules and variable *Escherichia coli*-derived rhBMP-2 dose. *Spine J.* 2014;14:1758-1768.
 28. Guigui P, Plais PY, Flautre B, et al. Experimental-model of posterolateral spinal arthrodesis in sheep 2 application of the model—evaluation of vertebral fusion obtained with coral (porites) or with a biphasic ceramic (triosite). *Spine (Phila. Pa. 1976).* 1994;19(24):2798-2803.
 29. Wheeler DL, Jenis LG, Kovach ME, Marini J, Turner AS. Efficacy of siliated calcium phosphate graft in posterolateral lumbar fusion in sheep. *Spine J.* 2007;7(3):308-317.
 30. Delawi D, Kruyt MC, Huipin Y, et al. Comparing autograft, allograft, and Tricalcium phosphate ceramic in a goat instrumented posterolateral fusion model. *Tissue Eng Part C Methods.* 2013;19(11):821-828.
 31. Brodsky AE, Kovalsky ES, Khalil MA. Correlation of radiologic assessment of lumbar spine fusions with surgical exploration. *Spine (Phila. Pa. 1976).* 1991;16(6 Suppl):S261-S265.
 32. Goldstein C, Drew B. When is a spine fused? *Injury.* 2011;42(3):306-313.
 33. Carreon LY, Djurasovic M, Glassman SD, Sailer P. Diagnostic accuracy and reliability of fine-cut CT scans with reconstructions to determine the status of an instrumented posterolateral fusion with surgical exploration as reference standard. *Spine (Phila. Pa. 1976).* 2007;32(8):892-895.
 34. Kotani Y, Cunningham BW, Cappuccino A, et al. The role of spinal instrumentation in augmenting lumbar posterolateral fusion. *Spine (Phila. Pa.).* 1996, 1976;21(3):278-287.
 35. Walsh WR, Loeffler A, Nicklin S, et al. Spinal fusion using an autologous growth factor gel and a porous resorbable ceramic. *Eur Spine J.* 2004;13(4):359-366.
 36. Alsaleh KAM, Tougas CA, Roffey DM, Wai EK. Osteoconductive bone graft extenders in posterolateral thoracolumbar spinal fusion: a systematic review. *Spine (Phila. Pa. 1976).* 2012;37(16):993-1000.
 37. Kadam A, Millhouse P, Kepler C, et al. Bone substitutes and expanders in spine surgery: a review of their fusion efficacies. *Int J Spine Surg.* 2016;10:33.
 38. Ghanaati S, Barbeck M, Detsch R, et al. The chemical composition of synthetic bone substitutes influences tissue reactions in vivo: histological and histomorphometrical analysis of the cellular inflammatory response to hydroxyapatite, beta-tricalcium phosphate and biphasic calcium phosphate cer. *Biomed Mater.* 2012;7(1):15005.
 39. Chen Y, Wang J, Zhu XD, et al. Enhanced effect of β -tricalcium phosphate phase on neovascularization of porous calcium phosphate ceramics: in vitro and in vivo evidence. *Acta Biomater.* 2015;11(1):435-448.
 40. Yuan H, Van Blitterswijk CA, De Groot K, De Bruijn JD. A comparison of bone formation in biphasic calcium phosphate (BCP) and hydroxyapatite (HA) implanted in muscle and bone of dogs at different time periods. *J Biomed Mater Res: Part A.* 2006;78(1):139-147.
 41. Wang J, Chen Y, Zhu X, et al. Effect of phase composition on protein adsorption and osteoinduction of porous calcium phosphate ceramics in mice. *J Biomed Mater Res - Part A.* 2014;102(12):4234-4243.
 42. Fariña NM, Guzón FM, Peña ML, Cantalapedra AG. In vivo behaviour of two different biphasic ceramic implanted in mandibular bone of dogs. *J Mater Sci.* 2008;19(4):1565-1573.
 43. Jensen SS, Bornstein MM, Dard M, et al. Comparative study of biphasic calcium phosphates with different HA/TCP ratios in mandibular bone defects. A long-term histomorphometric study in minipigs. *J Biomed Mater Res: Part B Appl Biomater.* 2009;90(B(1)):171-181.
 44. Gauthier O, Boulter JM, Aguado E, Pilet P, Daculsi G. Macroporous biphasic calcium phosphate ceramics: influence of macropore diameter and macroporosity percentage on bone ingrowth. *Biomaterials.* 1998;19(1-3):133-139.
 45. Klenke FM, Liu Y, Yuan H, et al. Impact of pore size on the vascularization and osseointegration of ceramic bone substitutes in vivo. *J Biomed Mater Res: Part A.* 2008;85(3):777-786.
 46. Galois L, Mainard D. Bone ingrowth into two porous ceramics with different pore sizes: an experimental study. *Acta Orthop Belg.* 2004;70(6):598-603.
 47. Li J, Zhi W, Xu T, et al. Ectopic osteogenesis and angiogenesis regulated by porous architecture of hydroxyapatite scaffolds with similar interconnecting structure in vivo. *Regen Biomater.* 2016;3(5):285-297.
 48. Mastrogiacomo M, Scaglione S, Martinetti R, et al. Role of scaffold internal structure on in vivo bone formation in macroporous calcium phosphate bioceramics. *Biomaterials.* 2006;27(17):3230-3237.
 49. Eggl PS, Muller W, Schenk RK. Porous hydroxyapatite and tricalcium phosphate cylinders with two different pore size ranges implanted in

- the cancellous bone of rabbits. A comparative histomorphometric and histologic study of bony ingrowth and implant substitution. *Clin Orthop Relat Res.* 1988;232:127-138.
50. Bai F, Wang Z, Lu J, et al. The correlation between the internal structure and vascularization of controllable porous bioceramic materials *In Vivo* : a quantitative study. *Tissue Eng Part A.* 2010;16(12):3791-3803.
51. Kobayashi M, Nakamura T, Okada Y, et al. Bioactive bone cement: comparison of apatite and wollastonite containing glass-ceramic, hydroxyapatite, and β -tricalcium phosphate fillers on bone- bonding strength. *J Biomed Mater Res.* 1998;42:223-237.
52. Ogle ME, Segar CE, Sridhar S, Botchwey EA. Monocytes and macrophages in tissue repair: implications for immunoregenerative biomaterial design. *Exp Biol Med.* 2016;241(10):1084-1097.
53. Murray PJ, Allen JE, Biswas SK, et al. Macrophage activation and polarization: nomenclature and experimental guidelines. *Immunity.* 2014;41(1):14-20.

How to cite this article: van Dijk LA, Duan R, Luo X, et al. Biphasic calcium phosphate with submicron surface topography in an *Ovine* model of instrumented posterolateral spinal fusion. *JOR Spine.* 2018;1:e1039. <https://doi.org/10.1002/jsp2.1039>